Nano Research 2014, 7(9): 1364–1369
DOI 10.1007/s12274-014-0501-4
Research Article

ISSN 1998-0124
CN 11-5974/O4

Hydroformylation of alkenes over rhodium supported on the metal–organic framework ZIF-8

Chao Hou, Guofeng Zhao, Yongjun Ji, Zhiqiang Niu, Dingsheng Wang, and Yadong Li (✉)

Department of Chemistry, Tsinghua University, Beijing 100084, China

Received: 7 April 2014
Revised: 20 May 2014
Accepted: 25 May 2014

© Tsinghua University Press and Springer-Verlag Berlin Heidelberg 2014

KEYWORDS

heterogeneous catalysis,
supported rhodium catalyst,
metal–organic framework,
ZIF-8,
hydroformylation

ABSTRACT

A highly porous and crystalline metal–organic framework (MOF) ZIF-8 has been synthesized and used for the preparation of a supported rhodium nanoparticle catalyst (Rh@ZIF-8). The material has been characterized by PXRD, TEM, EDX, ICP–AES and nitrogen adsorption. The catalytic properties of Rh@ZIF-8 have been investigated in the hydroformylation of alkenes, with different chain length and structure, to give the corresponding aldehydes, and showed high activity. Furthermore, after the reaction was complete, the catalyst could be easily separated from the products by simple decantation and reused five times without a significant decrease in the activity under the investigated conditions.

The hydroformylation or oxo reaction employed for the synthesis of aldehydes and alcohols starting from alkenes is an important reaction from both industrial and academic perspectives [1–5]. All current commercial hydroformylation processes are based on homogeneous catalysts, mostly using rhodium complexes, which have supplanted cobalt derivatives due to their higher activity [3–5]. These processes also use phosphine or phosphite ligands to increase the regioselectivity towards the desired linear or branched aldehyde [6–14]. Although homogeneous catalysts give high conversion and selectivity for desired product in short reaction times, they suffer from the problems of separating the catalyst from the reaction mixture and catalyst recycling. Thus, the development of a successful heterogeneous catalyst would allow a much simpler industrial production process to be implemented. Research efforts are directed towards the heterogenization of rhodium/cobalt complexes for hydroformylation of alkenes. The attachment of homogeneous catalysts to polymeric organic, inorganic or hybrid supports are such examples [15–20]. Although such catalysts can be recycled and easily separated from the reaction mixtures, they are usually

Address correspondence to ydli@mail.tsinghua.edu.cn

significantly less catalytically active and less thermally stable than their homogeneous analogues and also require complicated synthesis procedures [21]. Thus the development of a practical heterogeneous catalyst, such as supported rhodium nanoparticle catalysts, is highly desirable.

Metal–organic frameworks (MOFs) are a new class of hybrid porous materials assembled with metal cations and organic ligands. By controlling the size and functionalization of the organic linkers, well-defined MOF structures with high surface areas and tunable pore sizes can be achieved, thus offering advantages over traditional microporous and mesoporous inorganic materials [22–26]. Owing to their high surface area and porosity, the uses of MOFs as supports for metal (e.g., Pd, Au, Ru, and Pt) nanoparticles (NPs) have recently received tremendous attention [27–32]. Furthermore, some NPs@MOFs have exhibited excellent catalytic activities in organic reactions due to the confinement effect of the substrate in a MOF which means the particles remain constrained and do not grow further after catalytic reactions [31–34]. By virtue of its high chemical and thermal stability (550 °C in N_2) and large surface area (ranging from 1,100 to 1,810 $m^2 \cdot g^{-1}$), ZIF-8 ($Zn(mim)_2$, mim = 2-methylimidazolate), a zeolite-type MOF, has become the most promising candidate as an effective matrix to control the particle size of NPs and improve their catalytic surface area for heterogeneous catalysis [35–39]. Herein, a highly porous and crystalline MOF ZIF-8 has been synthesized and used for the preparation of a supported rhodium nanoparticle catalyst. The material has been characterized by XRD, TEM, EDX, ICP–AES and nitrogen adsorption. The catalytic properties of Rh@ZIF-8 have been investigated in the hydroformylation of alkenes with different chain length and structure to the corresponding aldehydes, and showed high activity. It is worth noting that the Rh@ZIF-8 catalyst can be separated easily by filtration after reaction and be reused several times without significant loss in activity.

ZIF-8 was synthesized according to the reported method [35]. The synthesized ZIF-8 was activated and then added to a solution of $RhCl_3$ under vigorous agitation. The mixture was then reduced with freshly prepared aqueous $NaBH_4$ solution at 273 K. The solid was centrifuged and washed with three times with EtOH, and the resulting Rh@ZIF-8 was dried under vacuum (more details are given in the Electronic Supplementary Material (ESM)). The PXRD patterns of the synthesized ZIF-8 and Rh@ZIF-8 are similar to the simulated pattern of ZIF-8 (Fig. 1) reported by Yaghi et al. [36]. Both materials have high crystallinity and the sharp and strong peaks at 5–10° reveal the presence of micropores. The XRD pattern of Rh@ZIF-8 (Fig. 1(c)) did not show the characteristic diffraction peaks of rhodium metal, suggesting that the rhodium nanoparticles are finely dispersed. An alternative explanation is that the signal is below the detection limit because of the relatively low Rh loading [40]. In addition, the XRD pattern of Rh@ZIF-8 after reaction showed that the main diffraction peaks were consistent with those of pristine ZIF-8, indicating that the framework of ZIF-8 was maintained during the process of catalytic hydroformylation (Fig. 1(d)).

N_2 sorption isotherms of both samples are of type I (Fig. 2). The pore volumes of ZIF-8 and Rh@ZIF-8 calculated from their adsorption isotherms are 0.592 and 0.506 $cm^3 \cdot g^{-1}$, respectively. The decrease in pore volume (about 0.086 $cm^3 \cdot g^{-1}$) suggests that Rh enter through the pore windows and partially occupy the pores. The calculated BET surface areas of ZIF-8 and Rh@ZIF-8 are 1,366 and 1,178 $m^2 \cdot g^{-1}$, respectively. The reduction in surface area is also attributed to the incorporation of Rh in the pores of ZIF-8 [31, 32].

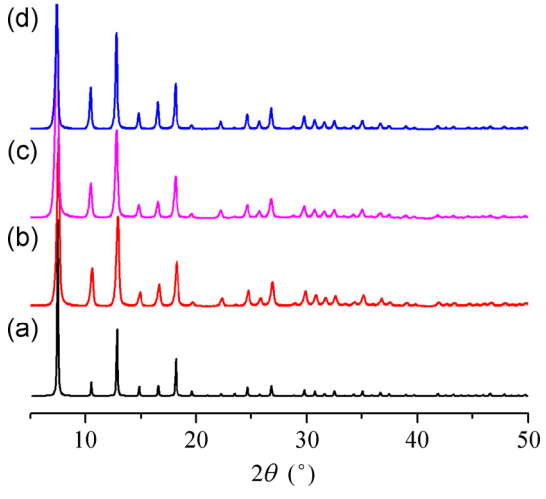

Figure 1 PXRD patterns of (a) simulated ZIF-8, (b) as-synthesized, (c) Rh@ZIF-8 and (d) the Rh@ZIF-8 after reaction.

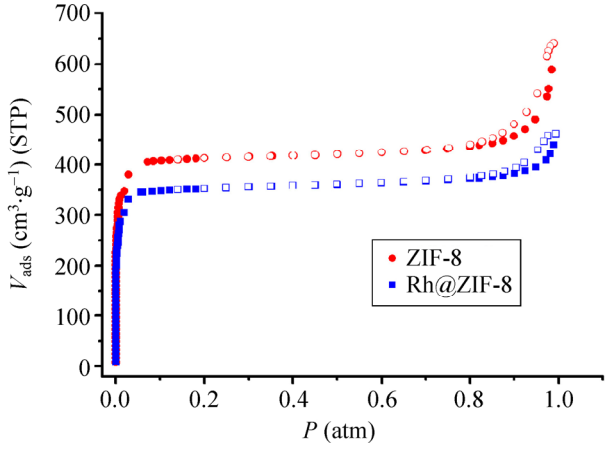

Figure 2 N_2 sorption isotherms of as-synthesized ZIF-8 and Rh@ZIF-8. Filled and open symbols represent adsorption and desorption branches, respectively.

To determine the particle size distribution, we conducted TEM analysis on Rh@ZIF-8. Figure 3 shows typical TEM images of Rh@ZIF-8. The low magnification image (Fig. 3(a)) shows the morphology of ZIF-8, but could not clearly show the Rh NPs, which indicate that the ZIF-8 immobilized Rh NPs were highly dispersed and have small sizes. The EDS of the sample shows the presence of Rh (Fig. S1 in the ESM). High-annular dark-field scanning TEM (HAADF-STEM) (Fig. 3(b)) provides direct evidence that the highly dispersed Rh NPs have been effectively immobilized by ZIF-8 and constrained to have small sizes. Clearly, the microporous structure of ZIF-8 favors the formation of small rhodium nanoparticles, probably due to a high dispersion of the precursor Rh^{3+} ions through weak π-interaction with the 2-methylimidazole linkers [31].

Catalytic activity of the Rh@ZIF-8 catalyst was evaluated in the hydroformylation of linear alkenes

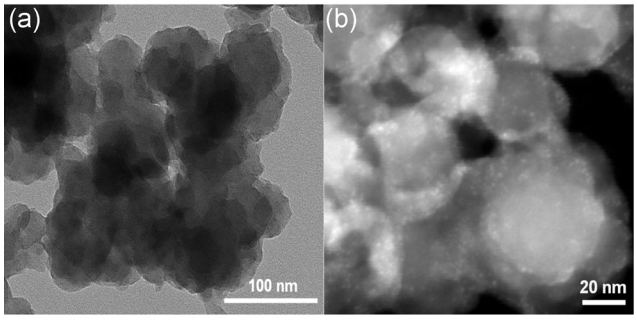

Figure 3 (a) TEM image and (b) HAADF-STEM image of Rh@ZIF-8.

with different chain lengths and structure, and the results are listed in Table 1. It should be noted that the analysis of the reaction products shows that beside n- and iso-aldehydes as the desired reaction products, double bond shifted internal alkenes are also formed as side products by isomerization. No significant hydrogenation of alkenes to saturated alkanes was observed. The blank experiments with n-hexene and n-octene show that the parent ZIF-8 (without rhodium) does not catalyze the double bond isomerization of n-alkenes to internal alkenes or the hydroformylation of alkenes to aldehydes even after reaction for 24 h of entry 3. The n/iso ratio of aldehydes was observed in the range of 0.4–0.9. Both the yield of aldehydes and the n/iso ratio are independent of carbon chain length of alkenes under our reaction conditions.

The effect of syngas pressure on the reaction was studied (Table 2). In the range from 1.0 to 5.0 MPa, as shown in Table 2 (entry 1 to entry 5), the aldehyde yield increased with increasing pressure and 81% aldehyde yield was achieved at 5.0 MPa. The n/iso ratio (0.6–3.0) obtained with the Rh@ZIF-8 catalyst was in agreement with the results reported by Dupont and co-workers using Rh nanoparticles [41].

It was also clear from the data in Table 2 that prolonged reaction time led to an increase in aldehyde yield (entry 5 to entry 9). It is worth noting that the yield of aldehydes increased sharply but the n/iso-ratio decreased when the reaction time was prolonged from 1 to 5 h (entry 5 to entry 9), which is in agreement with the results reported by Vu and co-workers [42, 43].

Table 1 Hydroformylation of different alkenes catalyzed by Rh@ZIF-8

Entry	Alkene	Yield of aldehydes (%)	Yield of iso[a] (%)	Yield of n[b] (%)	n/iso
1	1-Hexene	92	48	44	0.9
2	1-Heptene	87	58	29	0.5
3[c]	1-Heptene	0	0	0	0
4	1-Octene	86	51	35	0.7
5	1-Dodecene	76	41	35	0.9
6	1-Tetradecene	79	53	26	0.5
7	Styrene	94	68	26	0.4

[a]iso: Branched aldehydes; [b]n: Linear aldehydes; [c]catalyzed by ZIF-8, reaction time 24 h.

Table 2 Hydroformylation of 1-heptene catalyzed by Rh@ZIF-8

Entry	Pressure (MPa)	Time (h)	Yield of aldehydes (%)	Yield of iso[a] (%)	Yield of n[b] (%)	n/iso
1	1	5	8	2	6	3.0
2	2	5	21	7	14	2.0
3	3	5	39	19	20	1.1
4	4	5	52	29	23	0.8
5	5	5	81	50	31	0.6
6	5	1	21	5	16	3.2
7	5	2	44	25	19	0.8
8	5	3	55	31	24	0.8
9	5	4	74	43	31	0.7

[a] iso: Branched aldehydes; [b] n: Linear aldehydes.

The lifetime is an important aspect concerning the use of catalysts, and therefore the reusability of the Rh@ZIF-8 was examined (Fig. 4). After reaction, the catalyst was separated from the reaction solution by simple filtration in air after the reaction. The separated catalysts were all washed by isopropanol under ultrasonic washing and used in the next reaction run. The recovered Rh@ZIF-8 exhibited high catalytic efficiency without evident loss of activity after the catalyst was reused five times (Fig. 4). The stability of Rh@ZIF-8 may be due to the good dispersion of the Rh nanoparticles [44, 45].

In summary, highly dispersed Rh NPs with small particle sizes have been successfully immobilized in the frameworks of ZIF-8, and exhibit high catalytic activity for the hydroformylation of n-alkenes. Furthermore, after the reaction was completed, the catalyst could be easily separated from the products by simple decantation and reused five times without a significant decrease in activity under the investigated conditions. These highly efficient catalysts, which can be separated easily after reaction, represent a promising step toward the practical applications of MOFs as effective matrices to immobilize Rh NPs in the catalytic hydroformylation reaction system.

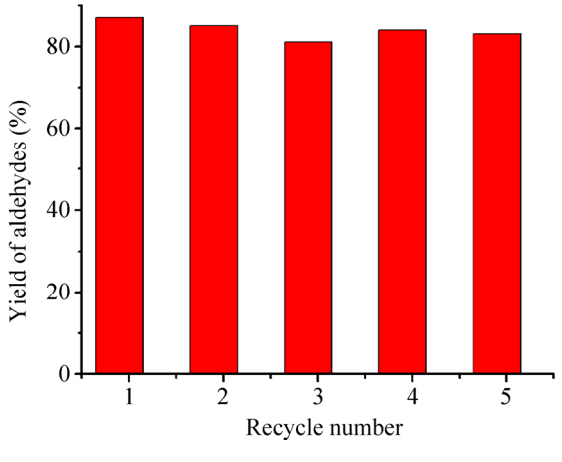

Figure 4 Reusability of Rh@ZIF-8 catalyst for hydroformylation of 1-heptene.

Acknowledgements

This work was supported by the State Key Project of Fundamental Research for Nanoscience and Nanotechnology (Nos. 2011CB932401, 2011CBA00500, and 2012CB224802), the National Natural Science Foundation of China (Nos. 21221062, 21131004, 21390393, 21171105, and 21322107), and the China Postdoctoral Science Foundation (No. 2013M540084).

Electronic Supplementary Material: Supplementary material (experimental procedures and energy dispersive X-ray spectrum of Rh@ZIF-8) is available in the online version of this article at http://dx.doi.org/10.1007/10.1007/s12274-014-0501-4.

References

[1] Franke, R.; Selent, D.; Börner, A. Applied hydroformylation. *Chem. Rev.* **2012**, *112*, 5675–5732.

[2] Metin, O.; Ho, S. F.; Alp, C.; Can, H.; Mankin, M. N.; Gultekin, M. S.; Chi, M. F.; Sun, S. H. Ni/Pd core/shell nanoparticles supported on graphene as a highly active and reusable catalyst for Suzuki–Miyaura cross-coupling reaction. *Nano Res.* **2013**, *6*, 10–18.

[3] Beller, M.; Cornils, B.; Frohning, C. D.; Kohlpaintner, C. W. Progress in hydroformylation and carbonylation. *J. Mol. Catal. A: Chem.* **1995**, *104*, 17–85.

[4] Chikkali, S. H.; Vlugt, J. I.; Reek, J. N. H. Hybrid diphosphorus ligands in rhodium catalysed asymmetric hydroformylation. *Coord. Chem. Rev.* **2014**, *262*, 1–15.

[5] Ungváry, F. Application of transition metals in hydroformylation annual survey covering the year 2006. *Coord. Chem. Rev.* **2007**, *251*, 2087–2102.

[6] Fernández, P. H.; Benet, B. J.; Vidal, F. A. Small bite-angle P–OP ligands for asymmetric hydroformylation and hydrogenation. *Org. Lett.* **2013**, *15*, 3634–3637.

[7] Selent, D.; Franke, R.; Kubis, C.; Spannenberg, A.; Baumann,

W.; Kreidler, B.; Börner, A. A new diphosphite promoting highly regioselective rhodium-catalyzed hydroformylation. *Organometallics* **2011**, *30*, 4509–4514.

[8] Doro, F.; Reek, J. N. H.; Leeuwen, P. W. N. M. Isostructural phosphine-phosphite ligands in rhodium-catalyzed asymmetric hydroformylation. *Organometallics* **2010**, *29*, 4440–4447.

[9] Worthy, A. D.; Joe, C. L.; Lightburn, T. E.; Tan, K. L. Application of a chiral scaffolding ligand in catalytic enantioselective hydroformylation. *J. Am. Chem. Soc.* **2010**, *132*, 14757–14759.

[10] Chikkali, S. H.; Bellini, R.; Bruin, B.; Vlugt, J. I.; Reek, J. N. H. Highly selective asymmetric Rh-catalyzed hydroformylation of heterocyclic olefins. *J. Am. Chem. Soc.* **2012**, *134*, 6607–6616.

[11] Wang, X.; Buchwald, S. L. Rh-catalyzed asymmetric hydroformylation of functionalized 1,1-disubstituted olefins. *J. Am. Chem. Soc.* **2011**, *133*, 19080–19083.

[12] Lightburn, T. E.; Paolis, O. A. D.; Cheng, K. H.; Tan, K. L. Regioselective hydroformylation of allylic alcohols. *Org. Lett.* **2011**, *13*, 2686–2689.

[13] Chen, C.; Qiao, Y.; Geng, H.; Zhang, X. A novel triphosphoramidite ligand for highly regioselective linear hydroformylation of terminal and internal olefins. *Org. Lett.* **2013**, *15*, 1048–1051.

[14] Dabbawala, A. A.; Bajaj, H. C.; Jasra, R. V. Rhodium complex of monodentate phosphite as a catalyst for olefins hydroformylation. *J. Mol. Catal. A: Chem.* **2009**, *302*, 97–106.

[15] Yoneda, N.; Nakagawa, Y.; Mimami, T. Hydroformylation catalyzed by immobilized rhodium complex to polymer support. *Catal. Today* **1997**, *36*, 357–364.

[16] Huang, L.; He, Y.; Kawi, S. Catalytic studies of aminated MCM-41-tethered rhodium complexes for hydroformylation of 1-octene and styrene. *J. Mol. Catal. A: Chem.* **2004**, *213*, 241–249.

[17] Riisager, A.; Wasserscheid, P.; Hal, R.; Fehrmann, R. Continuous fixed-bed gas-phase hydroformylation using supported ionic liquid-phase (SILP) Rh catalysts. *J. Catal.* **2003**, *219*, 452–455.

[18] Zhang, Y.; Nagasaka, K.; Qiu, X.; Tsubaki, N. Low-pressure hydroformylation of 1-hexene over active carbon-supported noble metal catalysts. *Appl. Catal. A: Gen.* **2004**, *276*, 103–111.

[19] Zhou, W.; He, D. A facile method for promoting activities of ordered mesoporous silica-anchored Rh–P complex catalysts in 1-octene hydroformylation. *Green Chem.* **2009**, *11*, 1146–1154.

[20] Zhou, W.; He, D. Lengthening alkyl spacers to increase SBA-15-anchored Rh–P complex activities in 1-octene hydroformylation. *Chem. Commun.* **2008**, 5839–5841.

[21] Sharma, S. K.; Parikh, P. A.; Jasra, R. V. Hydroformylation of alkenes using heterogeneous catalyst prepared by intercalation of $HRh(CO)(TPPTS)_3$ complex in hydrotalcite. *J. Mol. Catal. A: Chem.* **2010**, *316*, 153–162.

[22] Liu, N. A.; Yao, Y.; Cha, J. J.; McDowell, M. T.; Han, Y.; Cui, Y. Functionalization of silicon nanowire surfaces with metal-organic frameworks. *Nano Res.* **2012**, *5*, 109–116.

[23] Paz, F. A. A.; Klinowski, J.; Vilela, S. M. F.; Tomé, J. P. C.; Cavaleiro, J. A. S.; Rocha, J. Ligand design for functional metal–organic frameworks. *Chem. Soc. Rev.* **2012**, *41*, 1088–1110.

[24] Cohen, S. M. Postsynthetic methods for the functionalization of metal–organic frameworks. *Chem. Rev.* **2012**, *112*, 970–1000.

[25] O'Keeffe, M.; Yaghi, O. M. Deconstructing the crystal structures of metal–organic frameworks and related materials into their underlying nets. *Chem. Rev.* **2012**, *112*, 675–702.

[26] Cook, T. R.; Zheng, Y. R.; Stang, P. J. Metal–organic frameworks and self-assembled supramolecular coordination complexes: Comparing and contrasting the design, synthesis, and functionality of metal–organic materials. *Chem. Rev.* **2013**, *113*, 734–777.

[27] El-Shall, M. S.; Abdelsayed, V.; Khder, A. S.; Hassan, H. A.; El-Kaderi, H. M.; Reich, T. E. Metallic and bimetallic nanocatalysts incorporated into highly porous coordination polymer MIL-101. *J. Mater. Chem.* **2009**, *19*, 7625–7631.

[28] Jiang, H. L.; Akita, T.; Ishida, T.; Haruta, M.; Xu, Q. Synergistic catalysis of Au@Ag core–shell nanoparticles stabilized on metal−organic framework. *J. Am. Chem. Soc.* **2011**, *133*, 1304–1306.

[29] Yuan, B. Z.; Pan, Y. Y.; Li, Y. W.; Yin, B. L.; Jiang, H. F. A highly active heterogeneous palladium catalyst for the Suzuki–Miyaura and Ullmann coupling reactions of aryl chlorides in aqueous media. *Angew. Chem. Int. Ed.* **2010**, *49*, 4054–4508.

[30] Schröder, F.; Esken, D.; Cokoja, M.; van den Berg, M. W. E.; Lebedev, O. I.; Van Tendeloo, G.; Walaszek, B.; Buntkowsky, G.; Limbach, H. H.; Chaudret, B.; Fischer, R. A. Ruthenium nanoparticles inside porous $[Zn_4O(bdc)_3]$ by hydrogenolysis of adsorbed [Ru(cod)(cot)]: A solid-state reference system for surfactant-stabilized ruthenium colloids. *J. Am. Chem. Soc.* **2008**, *130*, 6119–6130.

[31] Dhakshinamoorthy, A.; Garcia, H. Catalysis by metal nanoparticles embedded on metal–organic frameworks. *Chem. Soc. Rev.* **2012**, *41*, 5262–5284.

[32] Moon, H. R.; Lim, D. W.; Suh, M. P. Fabrication of metal nanoparticles in metal–organic frameworks. *Chem. Soc. Rev.* **2013**, *42*, 1807–1824.

[33] Zhu, Q. L.; Li, J.; Xu, Q. Immobilizing metal nanoparticles

to metal−organic frameworks with size and location control for optimizing catalytic performance. *J. Am. Chem. Soc.* **2013**, *135*, 10210–10213.

[34] Zahmakiran, M. Iridium nanoparticles stabilized by metal organic frameworks (IrNPs@ZIF-8): Synthesis, structural properties and catalytic performance. *Dalton. Trans*. **2012**, *41*, 12690–12696.

[35] Huang, X. C.; Lin, Y. Y.; Zhang, J. P.; Chen, X. M. Ligand-directed strategy for zeolite-type metal–organic frameworks: Zinc(II) imidazolates with unusual zeolitic topologies. *Angew. Chem. Int. Ed.* **2006**, *45*, 1557–1559.

[36] Park, K. S.; Ni, Z.; Cote, A. P.; Choi, J. Y.; Huang, R. D.; Uribe-Romo, F. J.; Chae, H. K.; O'Keeffe, M.; Yaghi, O. M. Exceptional chemical and thermal stability of zeolitic imidazolate frameworks. *Proc. Natl. Acad. Sci. USA* **2006**, *103*, 10186–10191.

[37] Jiang, H. L.; Liu, B.; Akita, T.; Haruta, M.; Sakurai, H.; Xu, Q. Au@ZIF-8: CO oxidation over gold nanoparticles deposited to metal–organic framework. *J. Am. Chem. Soc.* **2009**, *131*, 11302–1303.

[38] Wang, P.; Zhao, J.; Li, X.; Yang, Y.; Yang, Q.; Li, C. Assembly of ZIF nanostructures around free Pt nanoparticles: Efficient size-selective catalysts for hydrogenation of alkenes under mild conditions. *Chem. Commun.* **2013**, *49*, 3330–3332.

[39] Li, P. Z.; Aranishi, K.; Xu, Q. ZIF-8 immobilized nickel nanoparticles: Highly effective catalysts for hydrogen generation from hydrolysis of ammonia borane. *Chem. Commun.* **2012**, *48*, 3173–3175.

[40] Hermannsdörfer, J.; Kempe, R. Selective palladium-loaded MIL-101 catalysts. *Chem. Eur. J.* **2011**, *17*, 8071–8077.

[41] Bruss, A. J.; Gelesky, M. A.; Machado, G.; Dupont, J. Rh(0) nanoparticles as catalyst precursors for the solventless hydroformylation of olefins. *J. Mol. Catal. A: Chem.* **2006**, *252*, 212–218.

[42] Vu, T. V.; Kosslick, H.; Schulz, A.; Harloff, J.; Paetzold, E.; Schneider, M.; Radnik, J.; Steinfeldt, N.; Fulda, G.; Kragl, U. Selective hydroformylation of olefins over the rhodium supported large porous metal–organic framework MIL-101. *Appl. Catal. A: Gen.* **2013**, *468*, 410–417.

[43] Vu, T. V.; Kosslick, H.; Schulz, A.; Harloff, J.; Paetzold, E.; Schneider, M.; Radnik, J.; Kragl, U.; Fulda, G.; Janiak, C.; Tuyen, N. D. Hydroformylation of olefins over rhodium supported metal-organic framework catalysts of different structure. *Micropor. Mesopor. Mater.* **2013**, *177*, 135–142.

[44] Zeng, Y.; Wang, Y.; Jiang, J.; Jin, Z. Rh nanoparticle catalyzed hydrogenation of olefins in thermoregulated ionic liquid and organic biphase system. *Catal. Commun.* **2012**, *19*, 70–73.

[45] Sun, Z.; Wang, Y.; Niu, M.; Yi, H.; Jiang, J.; Jin, Z. Poly(ethylene glycol)-stabilized Rh nanoparticles as efficient and recyclable catalysts for hydroformylation of olefins. *Catal. Commun*. **2012**, *27*, 78–82.